Biocompatible Nanogenerators through High Piezoelectric Coefficient $0.5Ba(Zr_{0.2}Ti_{0.8})O_3$-$0.5(Ba_{0.7}Ca_{0.3})TiO_3$ Nanowires for In-Vivo Applications

Miaomiao Yuan, Li Cheng, Qi Xu, Weiwei Wu, Suo Bai, Long Gu, Zhe Wang, Jun Lu, Huanping Li, Yong Qin, Tao Jing,* and Zhong Lin Wang**

Implantable medical devices (IMDs) have been widely used for therapies and may serve as functional devices to detect, prevent and cure many diseases challenging human life.[1–7] Among all factors affecting the performance of an IMD, a power source is indispensable for its operation, which is now becoming a major technological difficulty for sustainable operation of the IMD. Although several technologies such as battery, electromagnetic induction[8] and thermoelectric devices[9] have been explored, there are still many bottlenecks for them to power IMDs. Up to now, lithium batteries have been widely used to power the IMDs, but due to their limited capacity and lifetime, the patients are required to have surgeries to replace the depleted battery once a while, which is not only a painful process but also a high risky surgical procedure. As for the wireless power transmission technology, the energy is transferred between in vitro and in vivo coils or wires by electromagnetic wave or ultrasonic, which has a relatively low efficiency, high equipment cost, inconvenience to the patients and potential radiation effect.[10] In a case of the thermoelectric power generator, it is necessary to have a large temperature gradient, which is impossible inside human body. Therefore, it is extremely urgent to develop new techniques for effective and sustainable power supplies. Fortunately, there is abundant and natural in vivo biomechanical energy, such as bone strain, acceleration during locomotion, motion of respiration and heart contraction. If these mechanical energies can be harvested, it will contribute greatly to solving the challenge of powering IMDs.

The nanogenerators (NGs) as an emerging energy convertor,[11,12] which can convert tiny mechanical energy in the environment such as low frequency movement,[13,14] air flowing,[15] animal's motion[16] and heart beating[17] into electrical energy, have attracted much attention in recent years. NGs can be effectively integrated with the micro/nano-scale functional devices to form a self-powered system. This has been proven practicable via self-powered pH sensor, UV sensor, small liquid crystal display, commercial laser diode, pressure/speed sensor, environmental sensor and so on.[18–24] After generating electricity with rabbit quadriceps,[25] the piezoelectric NG shows the great potential to be further integrated with IMDs to form a self-powered system. Furthermore, piezoelectric NGs have been implemented in animals' bodies to harvest energy from the motion of different organisms such as heart, lung and diaphragm.[26] More importantly, comparing with the other energy technologies such as battery, NG can power the IMDs for quite long time because it can continuously convert the mechanical movements into electricity. As for the application of powering IMDs, the in vivo biocompatibility of NG is a big concern. Therefore, developing a kind of biocompatible NG with high performance is critically important. Although ZnO has a good biocompatibility,[27] due to the relatively low piezoelectric coefficient, the output power of ZnO based NGs is relatively low, which limits their applications in powering some in vivo electrical devices. The conventional high piezoelectric coefficient materials are dominated by the lead zirconatetitanate (PZT) family. However, the Pb toxicity causes severe pollution to the environment during the synthesis process and the hazard to human body, which hinders the applications of Pb-based materials for IMDs. Thus it is urgent to search for materials with high piezoelectric coefficient and good biocompatibility. As an emerging lead-free piezoelectric material, $0.5Ba(Zr_{0.2}Ti_{0.8})O_3$-$0.5(Ba_{0.7}Ca_{0.3})TiO_3$ (BZT-BCT) has a piezoelectric coefficient (~620 pC/N)[28] that can be compared with the conventional

M. Yuan,[+] L. Cheng,[+] Q. Xu, W. Wu, S. Bai, L. Gu, Z. Wang, Y. Qin
Institute of Nanoscience and Nanotechnology
School of Physical Science and Technology
Lanzhou University
Lanzhou 730000, China
E-mail: qinyong@lzu.edu.cn

M. Yuan, J. Lu, H. Li, T. Jing
Institute of Pathogenic Biology
School of Basic Medical Sciences
Lanzhou University
730000, China
E-mail: jtao@lzu.edu.cn

M. Yuan, Y. Qin, T. Jing
The Research Institute of Biomedical Nanotechnology
School of Basic Medical Sciences
Lanzhou University
Lanzhou 730000, China

Y. Qin, Z. L. Wang
Beijing Institute of Nanoenergy and Nanosystems
Chinese Academy of Sciences
Beijing 100085, China
E-mail: zhong.wang@mse.gatech.edu

Z. L. Wang
School of Materials Science and Engineering
Georgia Institute of Technology
Atlanta, Georgia 30332–0245, USA

[+]These authors contributed equally to this work.

DOI: 10.1002/adma.201402868

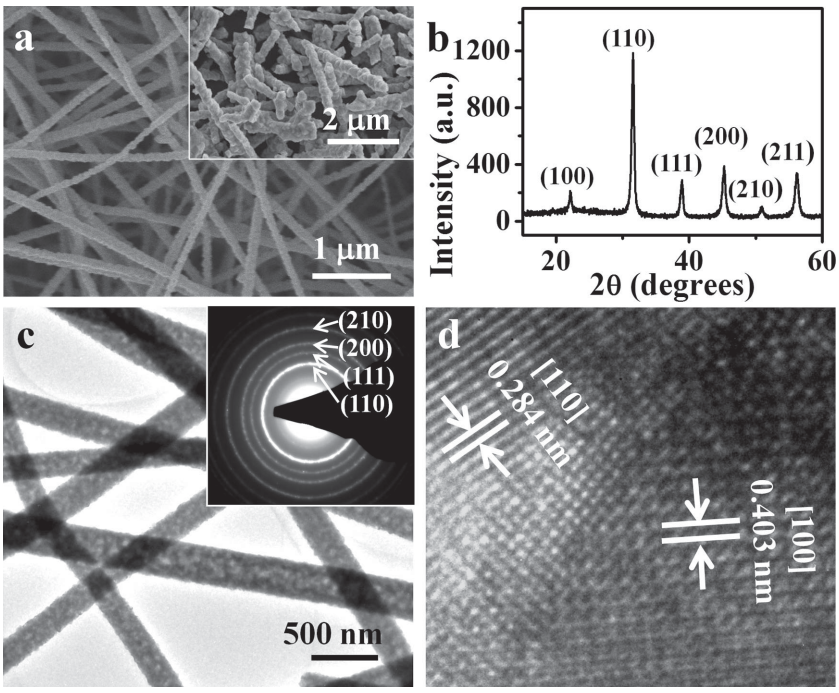

Figure 1. Structural characterization of BZT-BCT NWs. (a) SEM image of the milled BZT-BCT NWs. (b) XRD pattern of the sample. (c) TEM image of BZT-BCT NWs. The inset is a SAED pattern image. (d) HRTEM image of a BZT-BCT NW.

PZT family (200–710 pC/N).[29,30] So it is necessary to verify the biocompatibility of BZT-BCT nanowires (NWs) and its potential for fabricating biocompatible NGs.

In this paper, we fabricated BZT-BCT NWs by electrospinning method,[31] and examined the biocompatibility of BZT-BCT NWs by 3-(4,5)-dimethylthiahiazo(-z-y1)-3,5-di-phenytetrazoliumromide (MTT) assay, laser scanning confocal microscope (LSCM), and scanning electron microscope (SEM). The Chang liver cells and L929 cells could grow well in culture solution with BZT-BCT NWs and on the surface of a film composed with BZT-BCT NWs, respectively. Furthermore, we fabricated a biocompatible NG based on the BZT-BCT NWs. The Chang liver cells could grow well on the surface of the whole device and the in vivo experiments further confirmed the biocompatibility of the entire NG.

The BZT-BCT NWs were synthesized via a two-step process: electrospinning and subsequent calcinating. As the SEM image shown in **Figure 1**a, the diameters of BZT-BCT NWs are 210 ± 50 nm approximately, and the NWs were grinded in an agate mortar to nanorods with lengths ranging from 0.2 to 5 μm (Figure 1a, inset) in order to disperse uniformly in the culture solution. X-ray diffraction (XRD) spectrum of the synthesized BZT-BCT NWs is shown in Figure 1b, the BZT-BCT NWs are well crystallized and all their peaks can be indexed according to the reported tetragonal structure of BZT-BCT. Transmission electron microscope (TEM) (Figure 1c), selected area electron diffraction (SAED) (Figure 1c, inset) and the high-resolution TEM (HRTEM) image (Figure 1d) of the BZT-BCT NWs further demonstrated that the NWs are polycrystalline with tetragonal structure. Detail of the synthesis of BZT-BCT NWs is shown in the supporting information.

In this work, the cytotoxicity of the BZT-BCT NWs was preliminarily studied by MTT assay. First, the Chang liver cells and L929 cells were cultured in culture solution with BZT-BCT NWs (concentrations of BZT-BCT NWs were 0, 0.1, 1, 10 and 100 μg/mL), the relative viability of the cells were studied by MTT assay. The viability of the Chang liver cells cultured in these solutions for 24, 48 and 72 h, respectively, is shown in **Figure 2**a, the viability of the cells was higher than 96% after being cultured in the solution with BZT-BCT NWs' concentration lower than 1 μg/mL. The viability decreased slightly with the increasing of NW's concentration, but its value was still as high as 71% at the concentration of 100 μg/mL. The viability of the L929 cells shown in Figure 2b exhibits similar result as the Chang liver cells and the viability was 75% after being cultured in solution with 100 μg/mL NWs for 72 h. The reduction of viability might be induced by the gravity, limited space caused by the presence of nanomaterials and mechanical injuries of the cells. This study shows that within a large concentration range, BZT-BCT NWs have a slight influence on the growth of cells.

A detailed study was taken to detect the influence of the BZT-BCT NWs on the cellular morphology. Chang liver cells were cultured in culture solution with BZT-BCT NWs. And the cells' viability and the distribution of mitochondria in the cells were conducted via LSCM. As the images shown in **Figures 3**a–e, after being cultured in solution with BZT-BCT NWs for 48 h, the cells' morphology and the distribution of mitochondria in the cells showed no changes comparing with the cells in the control group. And the statistical result of the cells' density (Figure 3f) show a similar trend with the cells' viability getting by the MTT assay. The density of the cells decreased slightly

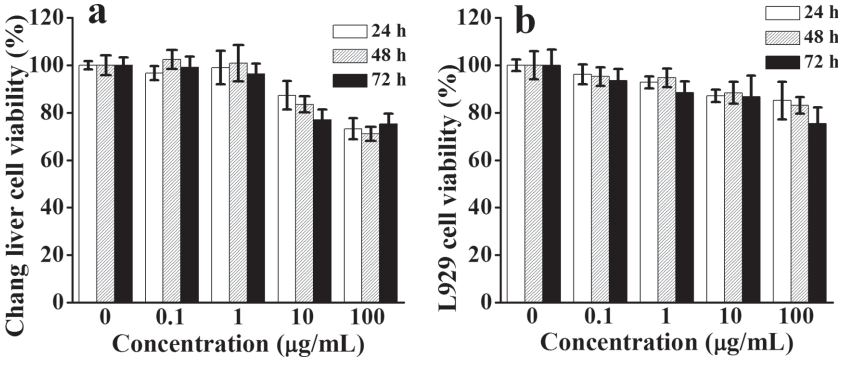

Figure 2. The viability of Chang liver cells (a) and L929 cells (b) tested by MTT assay as a function of BZT-BCT NW concentration and time. Error bars show standard deviations.

Adv. Mater. **2014**,
DOI: 10.1002/adma.201402868

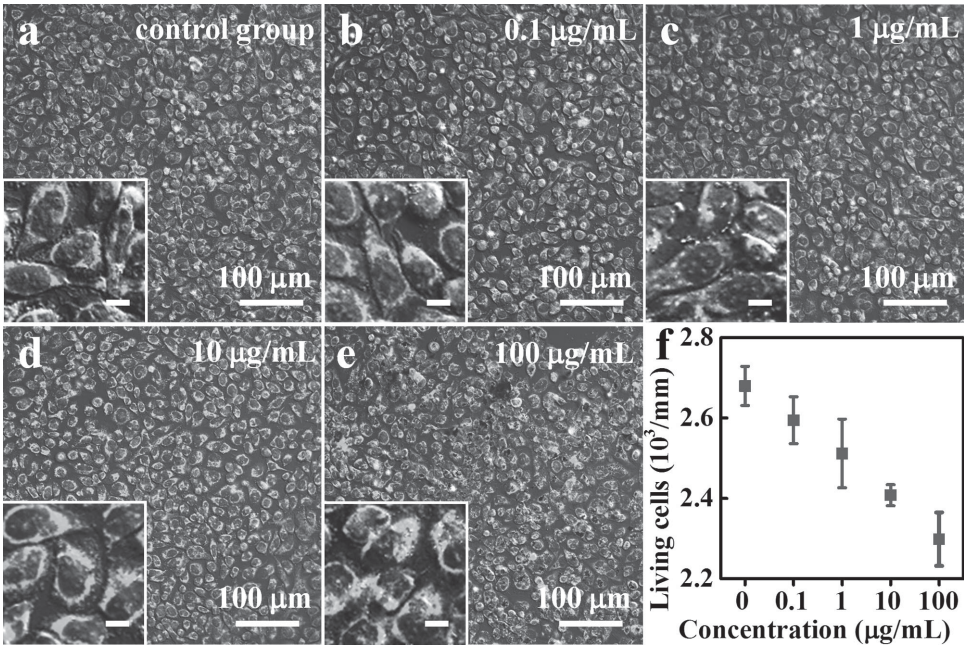

Figure 3. Observation of the cellular morphology, living numbers and the distribution of mitochondria in the cells. (a–e) LSCM images of Chang liver cells grown on the surface of cover slides cultured indifferent concentrations of BZT-BCT NWs. The inserts show the magnified images. The scale bars in the inserts are 10 μm. (f) Average density of Chang liver cells counted from the LSCM images with different BZT-BCT NWs concentrations. Error bars show standard deviations.

with the increasing of the NWs' concentration, and the percentage of living cells remained higher than 93% for the concentration lower than 1 μg/mL.

The detailed structure of the interface between the cells and BZT-BCT NWs was studied by SEM. As shown in **Figure 4**, the Chang liver cells which were cultured on the BZT-BCT NWs film (Figure 4a) for 48 h grew as well as the control group (Figure 4b) and the cells could adhere tightly to the NWs (Figure 4c). Even if the cell partly detached from the substrate, the NWs can still adhere tightly to the cell (shown in the yellow box of Figure 4c). These results indicate that the BZT-BCT NWs have no significant effect on the growth, morphology and structure of the cells, which demonstrate that the NWs are biocompatible.

Although NGs may be packaged in some biocompatible material such as poly-(dimethylsiloxane) (PDMS) to avoid the problem of their biocompatibility, potential risks could arise when the package material is corroded. So, it is essential to develop a NG with fully biocompatibility for powering the IMDs. Using the biocompatible BZT-BCT NWs mentioned above, we fabricated a partly packaged NG with the NWs bared (**Figure 5**a). After sterilized under UV light for 4 h, the NG was soaked into cell culture solution to testify whether the whole NG is biocompatible. Figure 5b shows the optical image of a NG with Chang liver cells on the surface, the cells attached to the NG were observed by metallographic microscopes with Janus Green B staining (1:5000). From the image,

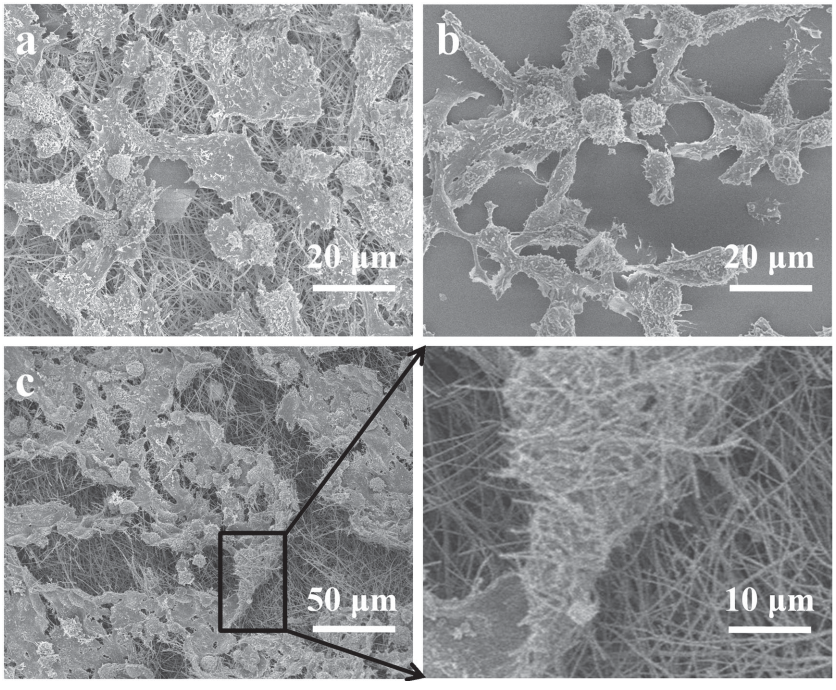

Figure 4. (a) SEM image of Chang liver cells grown on BZT-BCT NWs for 48 h. (b) SEM image of Chang liver cells grown on PET without BZT-BCT NWs for 48 h as a control group. (c) Details of the interface between cells and BZT-BCT NWs and the magnified image of the area marked in the yellow box.

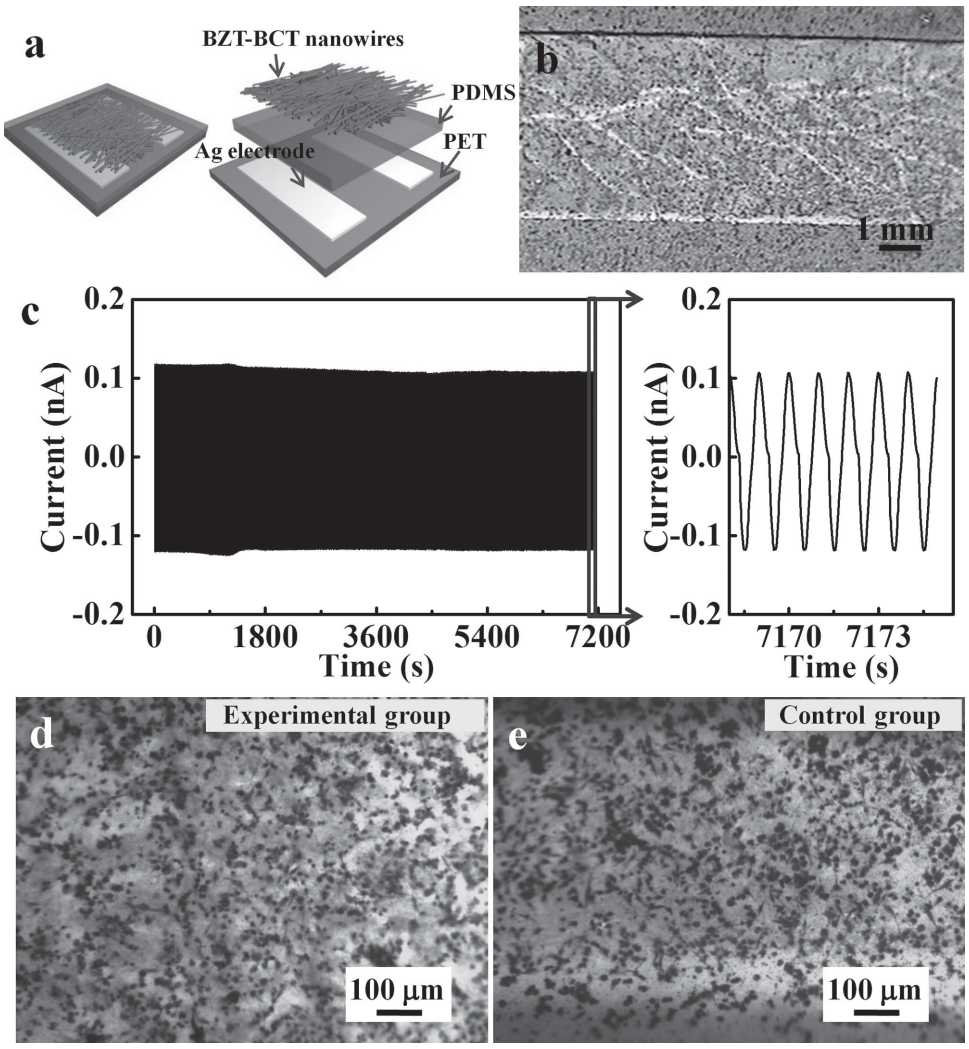

Figure 5. Investigation of the NG' biocompatibility in vitro. (a) Schematic of the biocompatible NG. (b) Optical image of the NG with Chang liver cells grown on it normally. The middle part with a light color is BZT-BCT film, while the dark part locating at the top and bottom are the electrode of the NG. (c) The current of the NG working for 2 h. (d) Optical image of the attached cells which were cultured for 24 h and exerted to stimulations via the NG for 2 h subsequently. (e) Optical image of the cells attached to NG cultured for 24 h as a control group.

we can see that the Chang liver cells could well grow on the whole NG. Furthermore, the NG was driven by a motor with an eccentric wheel through a wire fixed on the NG in the culture solution continuously for 2 h to check whether the mechanical movement and electrical signal (shown in Figure 5c) of the NG will damage the cells. The current and the voltage signal are tested by a current preamplifier (SR-570) and a voltage preamplifier (SR-560), respectively in the tests throughout the electric experiments, subsequently a switching polarity showed that the signals reversed their symbol after the device was reverse connected with the measurement system[32] (Figure S1), indicating that they are real signal generated by the NG. In addition, comparing with output of the NG with BZT-BCT NWs (0.3 V and 15 nA, shown in Figure S1), output of a device without BZT-BCT NWs (4 mV and 20 pA, shown in Figure S2) is very low, indicates that the outputs are indeed generated from the BZT-BCT nanowires. The experimental result shows that the NG could generate 0.12 nA current continuously with little attenuation in 2 hours' working. And as shown in Figure 5d and e, there were not obvious change to the density and morphology of the cells grown on the surface of the NG after 2 hours' operation. And the structure of the NG and the BZT-BCT NWs film also had not been damaged at all, which indicates the good biocompatibility and high robustness of the whole NG. In a word, the in vitro experiments fully prove that the NG possesses a good biocompatibility, biosafety and robustness, which eliminate the concern of the potential risks for future applications.

The above partly packaged NG was implanted subcutaneously into a rabbit's back to evaluate the in vivo biocompatibility (**Figure 6**a). Parts of BZT-BCT NWs were exposed to the surrounding tissue. By periodically pressing the back of the rabbit, the partly packaged NG could give an output current of 0.13 nA (Figure 6b). After 5 weeks, the rabbit was still live very well with the implanted NG. The NG with the surrounding tissue was then carefully taken out from the rabbit (Figure 6c), and the NG could be easily taken out from the

Adv. Mater. **2014**,
DOI: 10.1002/adma.201402868

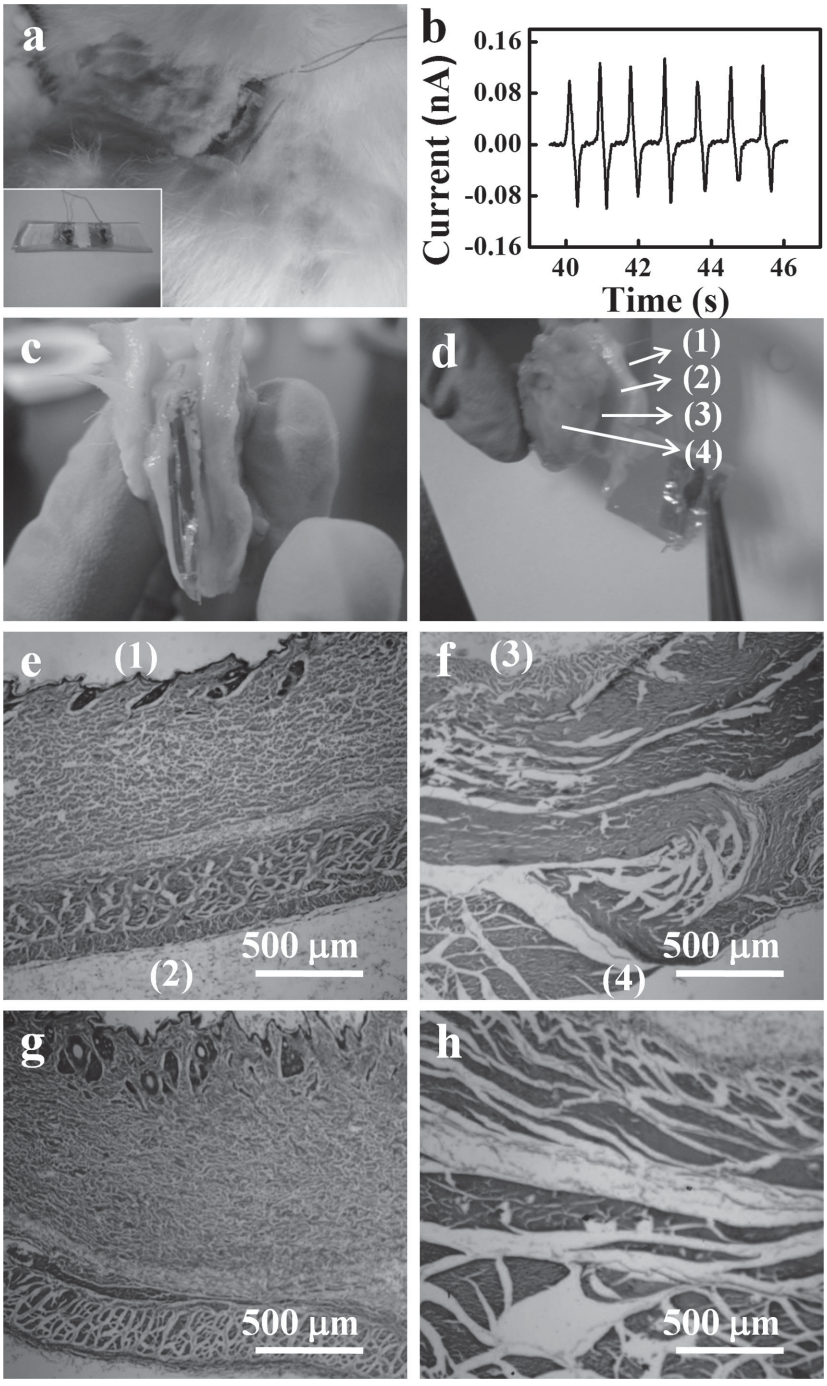

Figure 6. Investigation of the NG' biocompatibility in vivo. (a) Optical image of the biocompatible NG implanted in the rabbit's back. The insert shows the optical image of the NG. (b) The current of the NG in vivo. (c) The NG and the surrounding tissue. (d) The NG and the surrounding tissue were carefully separated. (e–h) The H&E stained images of rabbit's tissue. (e) The skin of the rabbit wich adjacent to one side of the NG corresponding to (1) and (2) in Figure 6d. (f) The muscle of the rabbit which adjacent to the other part of the NG corresponding to (3) and (4) in Figure 6d. (g) The skin of the rabbit as a control group. (h) The muscle of the rabbit as a control group.

attached tissue. Then, the surrounding tissue around the NG was sectioned and stained with haematoxylin and eosin (H&E). By observing the slices of tissue and comparing the tissue' morphology around the NG (Figures 6e–f) with that taken from areas far away from the NG (Figures 6g–h), no tissue damage, tearing, ballooning and neutrophil infiltration were found, which indicated there were no pathophysiological responses and injuries. Furthermore, this device could be driven by the slow walking of a rabbit and generate about 0.1 nA current (shown in Figure S3). This result further proves that the NG has a good biocompatibility for in vivo application. In a word, the BZT-BCT nanowire NG has the precious in vitro and in vivo bisosafety, which paves its way to potentially power in vivo devices.

In summary, the biocompatibility of lead-free BZT-BCT NWs with high piezoelectric coefficient has been studied and a kind of biocompatible NG has been successfully developed. After a thorough study of BZT-BCT NWs' biocompatibility with respect to Chang liver cells and L929 cells through MTT assay or LSCM, we found that they had good biocompatibility in bio-environment. On the basis of the BZT-BCT NWs, we fabricated a biocompatible NG with strong robustness. The in vitro experiments show that the Chang liver cells can grow normally on the surface of the NG, and the in vivo experiments of NG indicate that the NG have a good biocompatibility and biosafety. This new NG has a great potential for in vivo applications such as powering the IMDs.

Supporting Information

Supporting Information is available from the Wiley Online Library or from the author.

Acknowledgment

Research was supported by NSFC (NO. 51322203), NSFC (NO. 81171632), Fok Ying Tung education foundation (NO. 131044), PCSIRT (NO. IRT1251), the Fundamental Research Funds for the Central Universities (No. lzujbky-2014-m02, lzujbky-2013-k04, lzujbky-2013–34, lzujbky-2013–230), Special Talent Funding of Lanzhou University, and the "thousands talents" program for pioneer researcher and his innovation team, China. Adult rabbits (male, 2.5 kg) used for the experiments were purchased from the Laboratory Animal Center of lanzhou University , and our procedures in handling the animals were supervised by the Experimental Animal Ethics Committee of School of Basic Medical Sciences, Lanzhou University.

Received: June 28, 2014
Revised: August 24, 2014
Published online:

[1] B. J. Maron, W. K. Shen, M. S. Link, A. E. Epstein, A. K. Almquist, J. P. Daubert, G. H. Bardy, S. Favale, R. F. Rea, G. Boriani, N. A. M. Estes, P. Spirito, *New Engl. J. Med.* **2000**, *342*, 365–373.
[2] N. Bhadra, K. L. Kilgore, P. H. Peckham, *Med. Eng. Phys.* **2001**, *23*, 19–28.
[3] S. J. Rebscher, A. M. Hetherington, R. L. Snyder, P. A. Leake, B. H. Bonham, *J. Neurosci. Methods.* **2007**, *166*, 1–12.
[4] C. W. Scarantino, C. J. Rini, M. Aquino, T. B. Carrea, R. D. Ornitz, M. S. Anscher, R. D. Black, *Int. J. Radiat. Oncol. Biol. Phys.* **2005**, *62*, 606–613.
[5] Y. K. Song, W. R. Patterson, C. W. Bull, J. Beals, N. Hwang, A. P. Deangelis, C. Lay, J. L. McKay, A. V. Nurmikko, M. R. Fellows, J. D. Simeral, J. P. Donoghue, B. W. Connors, *IEEE. Trans. Neural. Syst. Rehabil. Eng.* **2005**, *13*, 220–226.
[6] H. Staecker, C. Jolly, C. Garnham, *Drug Discov. Today.* **2010**, *15*, 314–321.
[7] M. R. Sohail, D. Z. Uslan, A. H. Khan, P. A. Friedman, D. L. Hayes, W. R. Wilson, J. M. Steckelberg, S. Stoner, L. M. Baddour, *J. Am. Coll. Cardiol.* **2007**, *49*, 1851–1859.
[8] Y. Shigeta, T. Yamamoto, K. Fujimori, M. Sanagi, S. Nogi, T. Tsukagoshi, *Process of the 2nd European Wireless Technology Conference*. 28–29 September. **2009**, Rome, Italy.
[9] Y. Yang, X.-J. Wei, J. Liu, *J. Phys. D- Appl. Phys.* **2007**, *40*, 5790–5800.
[10] Z. Z. Qi, Z. J. Ling, L. Y. Hua, Y. J. Sheng, *2008 International Conference on Microwave and Millmeter Wave Technology Proceedings*. 21–24 April, **2008**, Nanjing, China.
[11] X. Wang, J. Zhou, J. Song, J. Liu, N. Xu, ZL. Wang, *Nano Lett.* **2006**, *6*, 2768–2772.
[12] Y. Qin, X. Wang, Z. L. Wang, *Nature.* **2008**, *451*, 809–813.
[13] J.-H. Lee, K. Y. Lee, M. K. Gupta, T. Y. Kim, D.-Y. Lee, J. Oh, C. Ryu, W. J. Yoo, C.-Y. Kang, S.-J. Yoon, J.-B. Yoo, S.-W. Kim, *Adv. Mater.* **2014**, *26*, 765–769.
[14] C. Sun, J. Shi, D. J. Bayerl, X. Wang, *Energy Environ. Sci.* **2011**, *4*, 4508–4512.
[15] K. Y. Lee, D. Kim, J.-H. Lee, T. Y. Kim, M. K. Gupta, S.-W. Kim, *Adv. Funct. Mater.* **2014**, *24*, 37–43.
[16] R. Yang, Y. Qin, C. Li, G. Zhu, Z. L. Wang, *Nano Lett.* **2009**, *9*, 1201–1205.
[17] Z. Li, G. Zhu, R. Yang, A. C. Wang, Z. L. Wang, *Adv. Mater.* **2010**, *22*, 2534–2537.
[18] S. Bai, Q. Xu, L. Gu, F. Ma, Y. Qin, Z. L. Wang, *Nano Energy.* **2012**, *1*, 789–795.
[19] W. Wu, S. Bai, M. Yuan, Y. Qin, Z. L. Wang, T. Jing, *ACS Nano.* **2012**, *6*, 6231–6235.
[20] Y. Hu, Y. Zhang, C. Xu, G. Zhu, Z. L. Wang, *Nano Lett.* **2010**, *10*, 5025–5031.
[21] S. Xu, B. J. Hansen, Z. L. Wang, *Nat. Commun.* **2010**, *1*, 93.
[22] S. Xu, Y. Qin, C. Xu, Y. Wei, R. Yang, Z. L. Wang, *Nat. Nanotechnol.* **2010**, *5*, 366–373.
[23] Y. Hu, C. Xu, Y. Zhang, L. Lin, R. L. Snyder, Z. L. Wang, *Adv. Mater.* **2011**, *23*, 4068–4071.
[24] M. Lee, J. Bae, J. Lee, C-S. Lee, S. Hong, Z. L. Wang, *Energy Environ. Sci.* **2011**, *4*, 3359–3363.
[25] B. E. Lewandowski, K. L. Kilgore, K. J. Gustafson, *Ann. Biomed. Eng.* **2009**, *37*, 2390–2401.
[26] C. Dagdeviren, B. D. Yang, Y. Su, P. L. Tran, P. Joe, E. Anderson, J. Xia, V. Doraiswamy, B. Dehdashti, X. Feng, B. Lu, R. Poston, Z. Khalpey, R. Ghaffari, Y. Huang, M. J. Slepian, J. A. Rogers. Proc. Natl. Acad. Sci. U.S.A. *Proc. Natl. Acad. Sci. U.S.A.* **2014**, *111*, 1927–1932.
[27] Z. Li, R. Yang, M. Yu, F. Bai, C. Li, Z. L. Wang, *J. Phys. Chem. C.* **2008**, *112*, 20114–20117.
[28] W. Liu, X. Ren, *Phys. Rev. Lett.* **2009**, *103*, 257602.
[29] T. R. Shrout, S. J. Zhang, *J. Electroceram.* **2007**, *19*, 113–126.
[30] G. H. Haertling, *J. Am. Ceram. Soc.* **1999**, *82*, 797–818.
[31] W. Wu, L. Cheng, S. Bai, W. Dou, Q. Xu, Z. Wei, Y. Qin, *J. Mater. Chem. A.* **2013**, *1*, 7332–7338.
[32] R. Yang, Y. Qin, C. Li, L. Dai, Z. L. Wang, *Appl. Phys. Lett.* **2009**, *94*, 022905.

Adv. Mater. **2014**,
DOI: 10.1002/adma.201402868